Talanta 94 (2012) 30–35

Contents lists available at SciVerse ScienceDirect

Talanta

journal homepage: www.elsevier.com/locate/talanta

A Pt layer/Pt disk electrode configuration to evaluate respiration and alkaline phosphatase activities of mouse embryoid bodies

Raquel Obregon[a], Yoshiko Horiguchi[a], Toshiharu Arai[a], Shihomi Abe[a], Yuanshu Zhou[a], RyosukeTakahashi[b], Akiko Hisada[b], Kosuke Ino[a], Hitoshi Shiku[a,*], Tomokazu Matsue[a,c,**]

[a] Graduate School of Environmental Studies, Tohoku University, 6-6-11, Aramaki, Aoba, Sendai 980-8579, Japan
[b] Advanced Research Laboratory, Hitachi Ltd., Hatoyama, Saitama 350-0395, Japan
[c] WPI Advanced Institute of Materials Research, Tohoku University, 2-1-1 Katahira, Aoba, Sendai 980-8577, Japan

ARTICLE INFO

Article history:
Received 21 November 2011
Received in revised form 27 January 2012
Accepted 30 January 2012
Available online 3 March 2012

Keywords:
Embryonic stem cell
Embryoid body
Respiration
Alkaline phosphatase
Scanning electrochemical microscopy
Pseudo reference electrode

ABSTRACT

A Pt layer/Pt disk electrode configuration was used as a scanning electrochemical microscopy (SECM) probe. The glass seal part of the insulator was covered with a Pt layer to form an exposed pseudo reference electrode. In a HEPES-based medium at pH 7.5, the half-wave potential ($E_{1/2}$) for $[Fe(CN)_6]^{4-}$ oxidation and O_2 reduction measured versus the internal Pt pseudo reference was shifted by about −0.2 V, compared with the $E_{1/2}$ measured versus the external Ag/AgCl reference electrode. The shape and the current of the cyclic voltammograms (CVs) did not change notably over time, indicating that the Pt layer is sufficiently stable to be used as an integrated pseudo reference for voltammetric measurements. To demonstrate the suitability for SECM applications, the Pt/Pt probe configuration was used for measuring the oxygen consumption and the alkaline phosphatase (ALP) activity of a single mouse embryoid body (mEB). Ten individual mEB samples were characterized to monitor the oxygen concentration profile. Oxygen reduction currents were monitored at −0.7 V versus the Pt pseudo reference and compared with those monitored at −0.5 V versus Ag/AgCl. The respiration rate of mEBs becomes greater with increasing cultivation dates. We have plotted the oxygen consumption rate ($F(O_2)$) of each mEB sample, measured versus the Pt layer and versus Ag/AgCl. The linearity of the plot was excellent (coefficient of determination $R^2 = 0.90$). The slope of the least squares method was 1. In a 1.0 mM *p*-aminophenylphospate (PAPP) HEPES buffer (pH 9.5) solution, APL activity of mEBs can be characterized, to monitor the *p*-aminophenol (PAP) oxidation current. ALP catalyzes the hydrolysis of PAPP to PAP. The $E_{1/2}$ for PAP oxidation measured versus the Pt layer was not shifted, compared with the $E_{1/2}$ versus Ag/AgCl. The mEB samples were characterized to monitor the PAP concentration profile. PAP oxidation currents were monitored at +0.3 V versus the Pt layer and compared with those monitored at +0.3 V versus Ag/AgCl. We have plotted the PAP production rate (F(PAP)) of each mEB sample, measured versus the Pt layer and versus Ag/AgCl. In this case, the linearity of the plot became slightly scattered, but it was found to be possible to evaluate ALP activities of mEB samples utilizing the Pt/Pt probe configuration. This type of probe is very useful because it is not necessary to insert a reference electrode into the measuring solution to obtain an electrical connection, and thus electrochemical measurement in a small volume becomes much easier.

1. Introduction

Scanning electrochemical microscopy (SECM) can be used with different types of probe (disk, ring, disk–ring, dual disk) and materials with sizes ranging from several micrometers to just a few nanometers. Microelectrodes have been fabricated from small diameter metal wires or carbon fibers sealed into tapered tips of pulled glass micropipettes and/or insulating polymers [1–11]. In the present study, the outer surface of the glass insulation of a disk-shaped microelectrode was sputtered with a Pt layer [12,13]. This is particularly useful because one does not then need to insert a reference electrode into a measuring solution in order to obtain an electrical connection, and electrochemical measurement in a small volume becomes much easier.

Miniaturization and microfabrication of reference electrodes play an important role in the development of integrated microsensors. Until now, 3-electrode configuration has generally been performed in a commercial 96-well plate, with a sample volume

* Corresponding author. Tel.: +81 22 795 7209; fax: +81 22 795 7209.
** Corresponding author at: Graduate School of Environmental Studies, Tohoku University, 6-6-11, Aramaki, Aoba, Sendai 980-8579, Japan. Tel.: +81 22 795 7209; fax: +81 22 795 7209.
E-mail addresses: shiku@bioinfo.che.tohoku.ac.jp (H. Shiku), matsue@bioinfo.che.tohoku.ac.jp (T. Matsue).

0039-9140/$ – see front matter © 2012 Elsevier B.V. All rights reserved.
doi:10.1016/j.talanta.2012.01.059

per well of 300 μL. Insertion of 3 electrodes into the well is possible [14,15], in order to electrochemically evaluate enzymatic activities. However, numerous problems are faced during miniaturization, most notably the rapid dissolution of the Ag/AgCl and the correspondingly short lifetime of the electrode [16]. The toxicity of Ag^+ can sometimes be significant when evaluating a biological sample [17], particularly for mammalian embryos and embryoid bodies.

We chose Pt because, after the base metal is deposited, an activation step is not necessary to generate the reference material. Conversely, in the case of Ag/AgCl, the silver layer must be chlorinated to produce the AgCl coating [18]. In contrast with other microelectrodes, our probe configuration, which integrates a pseudo reference electrode, improves the measurement procedure because it does not require an external Ag/AgCl, which often complicates the experimental design. This probe configuration allows for simplification of the measurement process, reduction of the assay time per sample, and high-throughput assays. To demonstrate the suitability of the Pt/Pt probe configuration, it was used as a scanning probe to measure the oxygen consumption and the alkaline phosphatase (ALP) activity of a single mouse embryoid body (mEB). The respiration activity of an embryoid body plays a crucial role not only in cellular viability but also in commitment to the differentiation lineage [19–21]. ALP activity is known to be an indicator of undifferentiated properties of embryonic stem cells [21]. We have applied the SECM system for quantitative characterization of respiration and ALP activity in individual mEBs. As it is not necessary to insert a reference electrode into the measuring solution to obtain an electrical connection, a high-throughput electrochemical measurement in a small volume (less than 5 nL) becomes much easier using the probe configuration (Fig. 1).

2. Materials and methods

2.1. Chemical reagents

p-Aminophenol (PAP, Wako Pure Chemical Industries), 2-[4-(2-hydroxyethyl)-1-piperazinyl] ethanesulfonic acid (HEPES; Dojindo Laboratories, Japan), fetal bovine serum (FBS; Gibco), and other chemicals were used as received. *p*-Aminophenylphosphate monosodium salt (PAPP) was purchased from LKT Lab Inc. or donated by Prof. Uichi Akiba from Akita University.

2.2. Cell culture

The hanging drop culture is the most widely used method for generating embryoid bodies, and involves the formation of an embryoid body by the aggregation of embryonic stem (ES) cells [22–24]. The mouse ES cell line was purchased from DS Pharma Biomedical. Co., Ltd., strain 129/SVEV, passage 11. The undifferentiated state was maintained in serum-free media (DS Pharma Biomedical Co., Ltd.) with 1000 U/mL of mouse leukemia inhibitory factor (LIF) and 1 mM β-mercaptoethanol. For the mEB formation culture, ES cells were dissociated and suspended in serum-free media with 15% FBS and 1 mM β-mercaptoethanol. Droplets of 20 μL of an ES cell suspension containing 2.5×10^4 cells/mL were placed in a 35 mm diameter dish. After 6 days of incubation at 37.5 °C in a water-saturated atmosphere of 95% air and 5% CO_2, single mEBs of between 200 and 300 μm in average diameter were formed.

2.3. Electrochemical measurement

The Pt disk microelectrode for the SECM experiment was fabricated according to the literature [25] as a working electrode. For the Pt/Pt probe integrating a Pt disk microelectrode and a Pt pseudo reference electrode, the Pt disk electrode was sputtered to form a 150 nm Pt layer (Anelva Corp.; L-232S-FH, RF200) outside the glass insulator. The outer Pt electrode layer was not covered with insulators, so as to gain a larger electrode area stabilizing the rest potential of the Pt layer electrode. The tip was carefully polished until a ring–disk electrode assembly was exposed.

Cyclic voltammograms (CVs) were obtained by controlling the potential of the probe-working electrode (Pt disk) versus the internal Pt layer integrated in the same probe, or an external Ag/AgCl reference electrode (Fig. 1A). A HEPES-based serum-free medium (ERAM2, Research Institute for the Functional Peptides), with or without 4 mM ferrocyanide, was selected for measuring the oxidation–reduction current.

2.4. Measurement of oxygen consumption

The oxygen reduction currents were monitored with a conventional Pt disk probe at −0.5 V versus Ag/AgCl or with a Pt/Pt probe at −0.7 V versus the internal Pt layer. A single mEB was transferred into a cell composed of 6 cone-shaped microwells with a 2 mm radius and a depth of 2 mm [26] (Research Institute for the Functional Peptides). When the mEB sample was transferred into a cone-shaped microwell, the sample fell to the bottom of the well and remained at the lowest point (Fig. 1A and S in Supplementary Data). A commercial SECM system, including the XYZ-stage (Suruga Seiki, K701-20R) and the potentiostat (HV405, Hokuto Denko), was controlled by a notebook computer (Fujitsu, FMV-BIBLO NE7/800). The details of the SECM system, including the definition of parameters, are shown in Supplementary Data and a previous report [26,27]. The electrode probe was scanned vertically from the side of the sample at z = 0–320 μm above (z = +320 μm), repeatedly up and down 6 times. The concentration profile formed near the sample has been confirmed to allow for spherical diffusion with the center of the sphere at the peak of the microwell cone (point P) rather than the center of the sample (point O). Therefore, the concentration profile was shown as a function of the distance (L) from point P. L can be obtained from the following equation:

$$L = \sqrt{(h+z)^2 + (r_s + r_{\min})^2} \quad (1)$$

where h is the distance between the peak of the cone-shaped microwell and the center of the sample (PO); r_s is the sample radius; and r_{min} is the distance between the tip center and the surface.

In a steady-state condition, the concentration profile for oxygen is expressed as follows:

$$C(L) = -\Delta C \left(\frac{L_s}{L}\right) + C^* \quad (2)$$

In this study, the ΔC value for oxygen is defined as the concentration difference (>0) between at $L = L_s$ and the bulk [26,28], where $L_s = h + r_s$. The oxygen consumption rate (F) was expressed as:

$$F = 2\pi \left(1 - \frac{1}{\sqrt{2}}\right) L_s D \Delta C \quad (3)$$

where D is the diffusion coefficient of oxygen (2.1×10^{-5} cm^2 s^{-1}) [26].

2.5. ALP activity

Following the culture of mEBs, the cone-shaped microwell was placed in 3 mL of a measuring solution containing 1.0 mM PAPP and HEPES-based saline solution (10 mM HEPES, 150 mM NaCl, 4.2 mM KCl, 2.7 mM $MgCl_2$, 1.0 mM $NaHPO_4$, and 11.2 mM glucose; pH 9.5). During the scans, the potential of the microelectrode was held at −0.3 V versus the Pt layer and versus Ag/AgCl, for facilitating the oxidation of PAP. The quantitative estimation of PAP produced from the mEB sample was basically the same as that shown for the oxygen consumption analysis. However, the ΔC value (>0) for PAP was

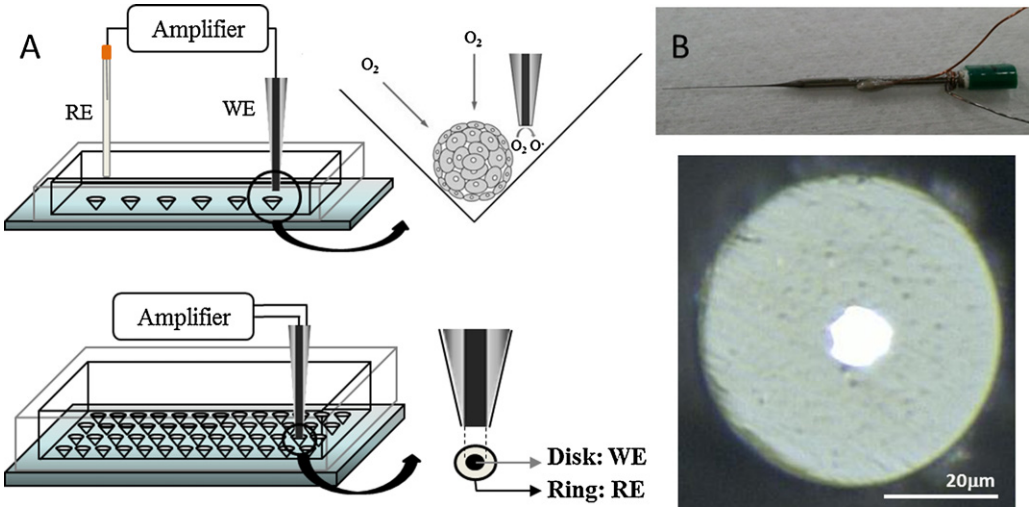

Fig. 1. (A) Scheme of the SECM measurement for a spherical sample located in a cone-shape microwell; system using a conventional Pt disk probe (top) and that using a Pt/Pt probe integrating a pseudo reference. (B) Photograph of a Pt/Pt probe (top) and tip of the Pt/Pt probe (bottom). The (b/a) value is 5.2.

defined as the subtraction of the PAP concentration at $L = L_S$ from the bulk PAP concentration. Eq. (2) was modified as follows:

$$C(L) = \Delta C \left(\frac{L_S}{L}\right) + C^* \qquad (2')$$

The diffusion coefficient of PAP was 7.1×10^{-6} cm^2 s^{-1} [29].

3. Results and discussion

The aim of this study was to fabricate and test a Pt/Pt probe featuring a Pt disk microelectrode and a Pt layer pseudo reference electrode. The probe was fabricated by sputtering a thin layer of Pt on to the outer surface of the glass insulation of a disk-shaped microelectrode. Typically, the radii of the disk and outer-ring electrodes were 4.6 and 23.8 μm, respectively. The ratio of the 2 radii (b/a; ring electrode radius (b) to disk electrode radius (a)) was 5.2. A photograph of the electrode (top) and a top view of the tip (bottom) of a Pt/Pt probe are shown in Fig. 1B.

Cyclic voltammetry was performed using an integrated pseudo reference to assess the Pt disk of the Pt/Pt probe as a microelectrode. ERAM2, with or without 4 mM $K_4Fe(CN)_6$, was selected as a measuring solution. Fig. 2A shows a CV of 4 mM $K_4Fe(CN)_6$ in ERAM2 that was recorded in a single cell with a Pt/Pt probe assembly with either the Pt layer as an internal pseudo reference (Pt) or an external reference (Ag/AgCl). The CV displayed the expected sigmoidal shape characteristic of microelectrodes. In this case, the CV for the set-up with the Pt pseudo reference was apparently shifted by −0.2 V, compared with the CV for the Ag/AgCl reference. This result means that the rest potential of the Pt layer is +0.2 V versus Ag/AgCl. In the presence of ferrocyanide/ferricyanide, the potential of the Pt layer electrode was controlled by the concentration ratio of ferrocyanide/ferricyanide. Even in the case of a solution containing a reduced form of the redox couple only, the resting potential of noble metal (e.g. Pt or Au) working electrodes does not significantly deviate from the formal potential of the redox [30]. A steady-state oxygen reduction current was obtained at −0.7 V versus the Pt layer. In preliminary studies, Pt layer/Pt disk electrodes with b/a values ranging from 1.75 to 6.6 were tested by comparing the limiting diffusion current of the Pt disk, before and after the deposition of Pt layer. Current fluctuation due to the interference (including redox cycling) between the Pt disk and Pt layer electrodes was observed in electrodes with b/a values ranging from 1.75 to 2.96 and was not observed in the (b/a) values ranging from 3.5 to 6.6. These (b/a) values are found to be large enough to omit redox cycling between the disk and the layer electrodes. These results are according to theoretical approach which indicates a strong tip response dependence on the (b/a) value [12,31,32].

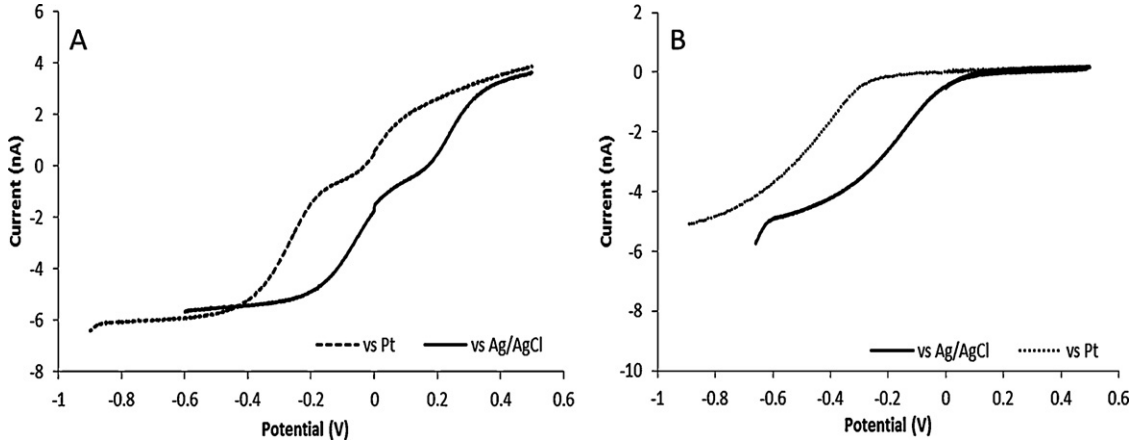

Fig. 2. Cyclic voltammograms in ERAM2 containing 4 mM $K_4Fe(CN)_6$ (A) and ERAM2 (B) recorded with a same Pt/Pt probe versus an internal Pt pseudo reference (dashed line) and versus an external reference Ag/AgCl electrode (solid line). Scan rate 20 mV s^{-1}. The (b/a) values were 5.2 (A) and 3.5 (B), respectively.

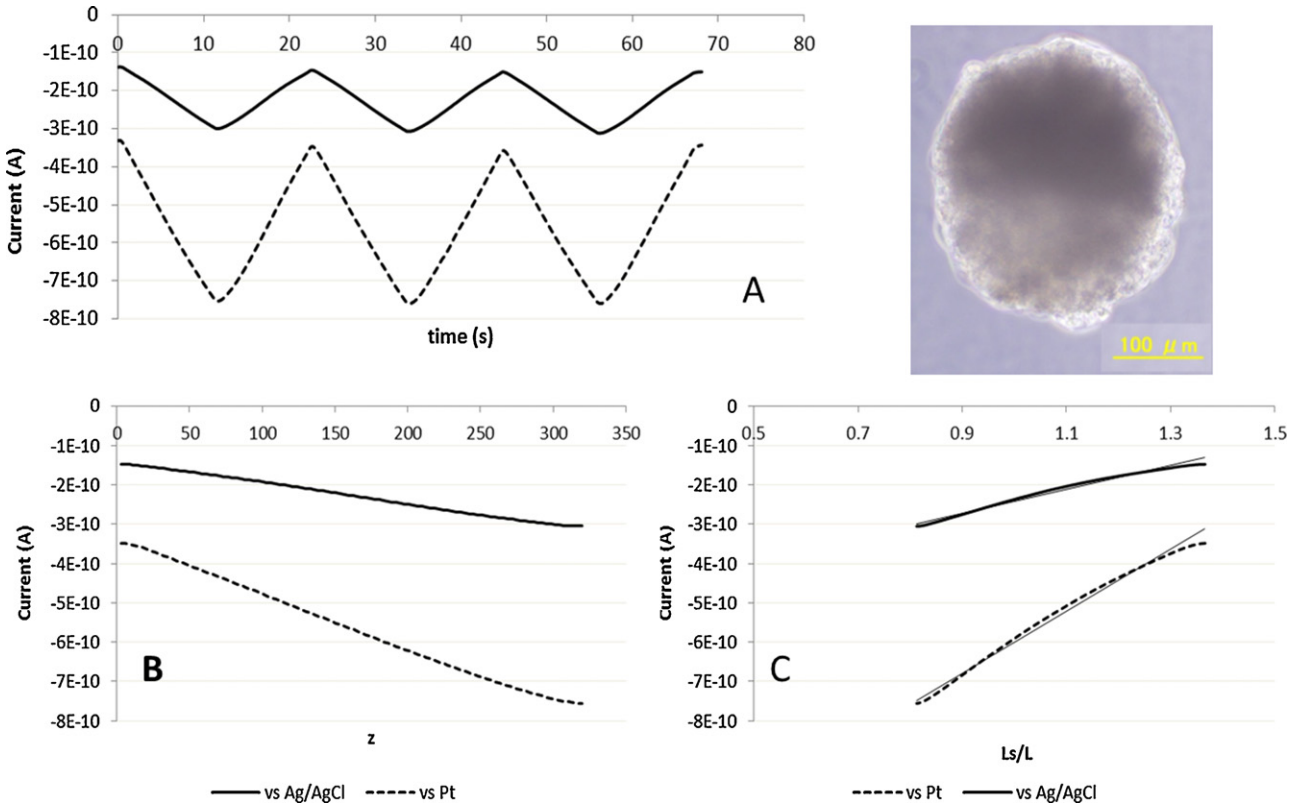

Fig. 3. (A) Photograph and time course of current profiles for mEB (day 6, r_s: 223 μm). Scale bar, 100 μm. (B) Current profiles as a function of z. (C) Current versus L_s/L plot. The R^2 was 0.99 (versus Pt pseudo reference) and 0.98 (versus Ag/AgCl). (A–C) Current was recorded with a Pt/Pt probe at −0.7 V versus an internal Pt pseudo reference (dashed line, Pt disk radius, 4.6 μm; the (b/a) value was 5.2) or with a conventional Pt disk probe at −0.5 V versus an external reference Ag/AgCl (solid line, Pt disk radius, 1.0 μm).

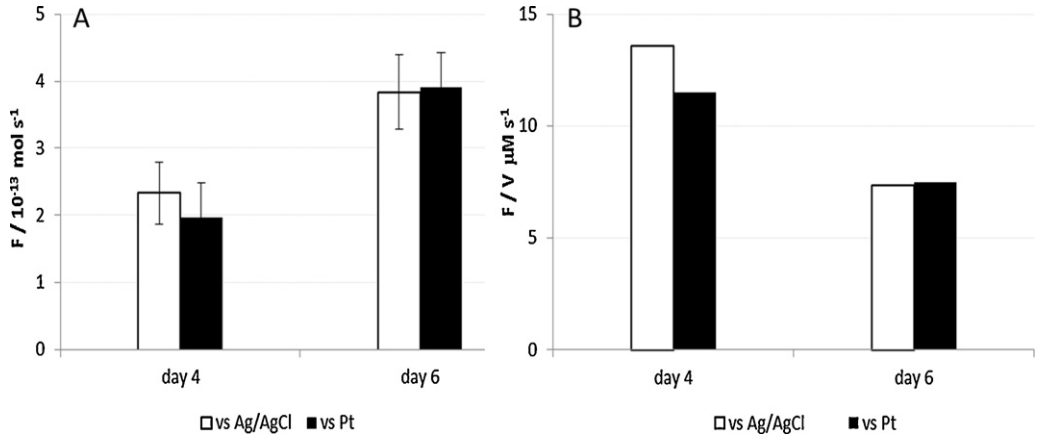

Fig. 4. Respiration rate, $F(O_2)$ (A) respiration rate per spheroid volume, $F(O_2)/V$ of mEB on day 4 and day 6 (B) measured at −0.7 V versus Pt pseudo reference (filled bars) and −0.5 V versus Ag/AgCl (blank bars); $N = 10$.

In the absence of ferrocyanide/ferricyanide couple, environmental condition including pH of solution becomes a major factor to stabilize the potential of the Pt layer electrode. The rest potential of the Pt layer was +0.4, +0.2, and +0.0 V versus Ag/AgCl at pH 4.1, 7.5, and 10.0, respectively. This result was accepted by the potential shift of the platinum oxide film/Pt couple with pH changes. The potential of the Pt layer electrode seems to be stabilized because of a relatively larger electrode area with the platinum oxide film on Pt. Fig. 2B shows a CV in ERAM2. The $E_{1/2}$ for O_2 reduction was shifted by about −0.2 V. If the microelectrode is compared for the oxidation of $[Fe(CN)_6]^{4-}$ measured versus Ag/AgCl, the value of I_{max} and $E_{1/2}$ does not change notably over time (~30 min), and neither does the sigmoidal shape.

To demonstrate the suitability of the Pt/Pt probe configuration for SECM applications, it was used for measuring the oxygen consumption and the ALP activity of a single mEB. Ten separate mEBs were characterized to monitor the oxygen concentration profile. Oxygen reduction currents were monitored with the Pt/Pt probe at −0.7 V versus the internal Pt layer and compared with the current profile monitored with a conventional Pt disk probe at −0.5 V versus an external Ag/AgCl electrode. In the present study, the oxygen consumption rate ($F(O_2)$) was quantified based on spherical

diffusion theory and the protocol developed previously [26]. Fig. 3A shows current profiles during a 3-times back-and-forth scanning of a single mEB (day 6, r_s: 223.5 μm) comparing the Pt layer and the Ag/AgCl electrode. A single measurement, completed within 64 s, recorded 6 current profiles, 3 up-scan (+z direction) and 3 down-scan (−z direction) by 320 μm. The tip scanning rate was 30 μm s^{-1}. The distance (r_{min}) between the tip center and the sample surface was typically 5–30 μm. At t = 0.0, 21.3, 42.7, and 64.0 s, the SECM tip located at z = 0.0 μm (where z is defined as the height from the center of the sample: see Fig. S2 in Supplementary data). On the other hand, at t = 10.7, 32.0, and 53.3 s, the tip located at z = 320 μm. Fig. 3B shows the current profile as a function of z. The reduction current (expressed as a negative value) decreased with smaller z value because the oxygen concentration near the sample became lower as a result of the respiration of mEBs. The oxygen concentration profile near the mEB was known to be allowed with a spherical diffusion with the distance (L) from point P, the top of the cone-shaped microwell. The appropriateness of adopting diffusion theory was confirmed by the current versus L_s/L plot shown in Fig. 3C. The coefficient of determination (R^2) of the 2 plots obtained at −0.7 V versus the Pt layer and at −0.5 V versus Ag/AgCl were 0.99 and 0.98, respectively, both indicating excellent linearity. Importantly, the $\Delta C(O_2)$ value obtained with the Pt layer was 1.17×10^2 μM, which was in very good accordance with that obtained with the Ag/AgCl reference (1.18×10^2 μM).

Next, we compare the value of $F(O_2)$ on day 4 and day 6. Fig. 4A shows the average of the respiration rate on days 4 and 6, measured at −0.7 V versus the Pt layer and compared with those monitored at −0.5 V versus Ag/AgCl. The $F(O_2)$ values increased by increasing the cultivation times. The respiration rate of the mEB becomes greater with increasing cultivation time. No significant difference was observed between the $F(O_2)$ values obtained with the Pt layer and the Ag/AgCl reference electrode. Fig. 4B shows the average of the respiration rate per volume of mEB (F/V). Over this time period, the F/V value decreased when increasing the cultivation time. In fact, the respiration activity inside the mEB became lower when the r_s became larger because of the deficiency of oxygen (hypoxia). Fig. 5 shows the values for oxygen consumption ($F(O_2)$) of each mEB sample measured versus the Pt layer and compared with the F value measured versus Ag/AgCl. The linearity of the plot was excellent (R^2 = 0.93). These results confirm the stability and robustness of our electrode. In both experiments, the values are similar, demonstrating that our electrode can be used as a scanning probe

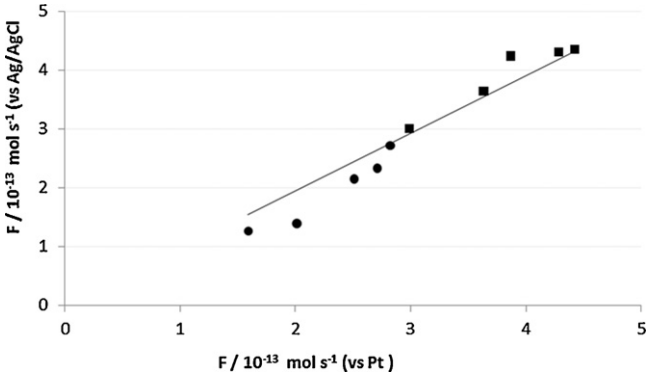

Fig. 5. Plot of the oxygen consumption ($F(O_2)$) values measured at −0.7 V versus the Pt pseudo reference and at −0.5 V versus Ag/AgCl. Circles and squares correspond to data for mEB of day 4 and day 6. The R^2 was 0.93.

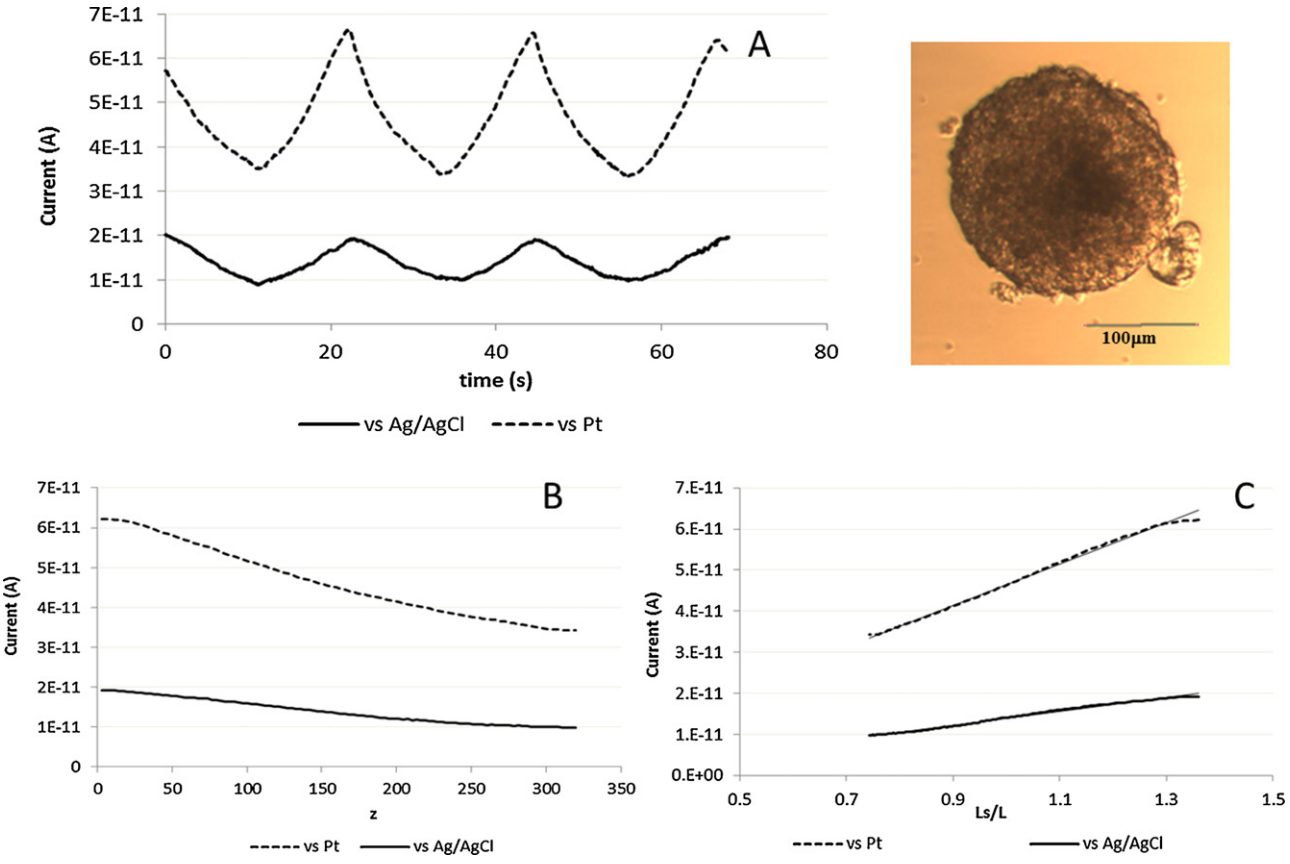

Fig. 6. (A) Photograph and time course of current profiles for mEB (day 6, r_s: 192.4 μm). Scale bar, 100 μm. (B) Current profiles as a function of z. (C) Current versus L_s/L plot. The R^2 was 0.99 (versus Pt pseudo reference) and 0.99 (versus Ag/AgCl). (A–C) Current was recorded with a Pt/Pt probe at +0.3 V versus an internal Pt pseudo reference (dashed line, Pt disk radius, 4.6 μm; the (b/a) value was 5.2) or with a conventional Pt disk probe at +0.3 V versus an external Ag/AgCl (solid line, Pt disk radius, 1.0 μm).

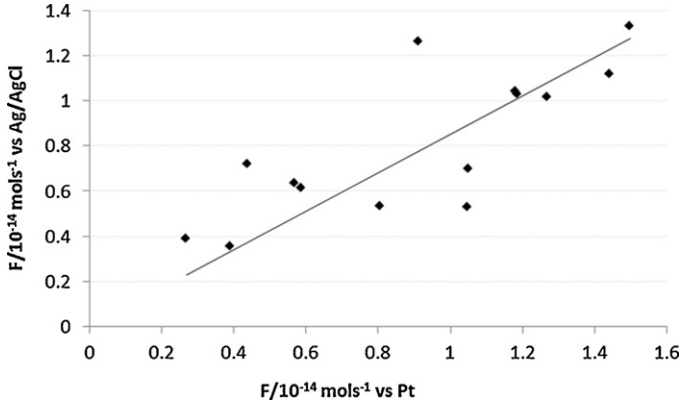

Fig. 7. Plot of F(PAP) values recorded at +0.3 V versus the Pt layer and +0.3 V versus Ag/AgCl. Data were obtained for mEBs at day 6. The R^2 was 0.58.

to measure the oxygen consumption without the need to use an external reference.

ALP hydrolyzes PAPP to PAP, which is an electrochemically active species [28]. The use of PAPP, instead of other ALP substrates, results in lower limits of determination (LODs), wider linear ranges, and a simpler methodology for the detection of the enzymatic product. Moreover, the applied potential for oxidation of PAP is lower than the potential for oxidation of other ALP substrates hydrolysis products, which reduces the number of potential interferences that can be oxidized at the electrode surface. CVs in HEPES-based saline solution were used for electrochemical oxidation of PAP and PAPP with the Pt/Pt probe, and a calibration curve for PAP concentration is shown in Fig. S2 in Supplementary Data. The $E_{1/2}$ for PAP oxidation measured versus the Pt layer was not shifted, compared with the case versus the external Ag/AgCl reference electrode. The calibration curves for the Pt/Pt probe and the conventional Pt disk probe were used to estimate local PAP concentration change.

Fourteen separate mEB samples were characterized to monitor ALP activity. PAP oxidation current was recorded with a Pt/Pt probe at +0.3 V versus the internal Pt pseudo reference electrode and with a conventional Pt disk electrode at +0.3 V versus the external Ag/AgCl electrode. Fig. 6A shows current profiles as a function of time during 3-times back-and-forth scanning of a single mEB (day 6, r_s: 192.4 μm). At z = 0.0 μm (t = 0.0, 21.3, 42.7, and 64.0 s), the PAP oxidation current (expressed as a positive value) increased because the PAP concentration near the sample became larger due to the endogenous ALP activity of mEB. Fig. 6B shows the current profile as a function of z. The PAP concentration profile near the mEB was expressed with spherical diffusion. The appropriateness of adopting diffusion theory was confirmed by the current versus L_s/L plot, shown in Fig. 6C. The R^2 of the 2 plots obtained with the Pt/Pt probe versus the internal Pt layer and with the conventional Pt disk probe versus the external Ag/AgCl electrode were 0.99 in both cases, indicating an excellent linearity. The ΔC(PAP) value obtained with the Pt layer was 8.25 μM, which was in very good accordance with that obtained with the Ag/AgCl reference (7.51 μM).

Fig. 7 shows the relationship between F(PAP) values versus the Pt layer and versus Ag/AgCl on day 6 of each mEB sample: coefficient of determination, R^2 = 0.58. In this case, the linearity of the plot becomes slightly scattered due to fouling and the instability of the products over the time (the half-life of PAP and PQI in alkaline media is low), but, basically, it was found to be possible to evaluate the ALP activity of an mEB sample utilizing the Pt/Pt electrode configuration. This type of electrode is particularly useful because it is not necessary to insert a reference electrode into the measuring solution to obtain an electrical connection, and thus electrochemical measurement in a small volume becomes much easier.

4. Conclusion

An integrated probe was fabricated, with working/pseudo reference electrodes, for practical oxygen consumption and PAP production measurement. The consumption pattern observed with the Pt layer/Pt disk electrode agreed well with that found by using the conventional SECM method. The Pt layer/Pt disk electrode improves the measurement procedure and enables rapid measurement of oxygen consumption. We believe that the probe integrating the Pt pseudo reference will improve the accessibility of electrochemistry with commercial multitier plates.

Acknowledgment

This research is partly supported by the Cabinet Office, Government of Japan, through its “Funding Program for Next Generation World-Leading Researchers” (H.S.).

Appendix A. Supplementary data

Supplementary data associated with this article can be found, in the online version, at doi:10.1016/j.talanta.2012.01.059.

References

[1] B.D. Pendley, H.D. Abruna, Anal. Chem. 62 (1990) 782.
[2] K.T. Kawagoe, J.A. Jankowski, R.M. Wightman, Anal. Chem. 63 (1991) 1589.
[3] T.G. Strein, A.G. Ewing, Anal. Chem. 64 (1992) 1368.
[4] G. Zhao, D.M. Giolando, J.R. Kirchhoff, Anal. Chem. 67 (1995) 2592.
[5] A. Schulte, R.H. Chow, Anal. Chem. 68 (1996) 3054.
[6] B.B. Katemann, T. Schuhmann, Electroanalysis 14 (2002) 22.
[7] C.G. Zoski, Electroanalysis 14 (2002) 1041.
[8] F. Turcu, A. Schulte, W. Schuhmann, Anal. Bioanal. Chem. 380 (2004) 736.
[9] Y. Takahashi, Y. Hirano, T. Yasukawa, H. Shiku, H. Yamada, T. Matsue, Langmuir 22 (2006) 10299.
[10] Y. Takahashi, A.I. Shevchuk, P. Novak, Y. Murakami, H. Shiku, Y.E. Korchev, T. Matsue, Am. Chem. Soc. J. 132 (2010) 10118.
[11] Y. Takahashi, A.I. Shevchuk, P. Novak, Y.J. Zhang, N. Ebejer, J.V. Macpherson, P.R. Unwin, A.J. Pollard, D. Roy, C.A. Clifford, H. Shiku, T. Matsue, D. Klenerman, Y.E. Korchev, Angew. Chem. Int. Ed. 50 (2011) 9638.
[12] S.L.R. Harvey, K.H. Parker, D. O'Hare, Electroanal. Chem. J. 610 (2007) 122.
[13] S.L.R. Harvey, P. Coxon, D. Bates, K.H. Parker, D. O'Hare, Sens. Actuators B 129 (2008) 659.
[14] W. Sun, K. Jiao, S.S. Zhang, C.L. Zhang, Z.F. Zhang, Anal. Chim. Acta 434 (2001) 43.
[15] K. Jiao, W. Sun, S.S. Zhang, G. Sun, Anal. Chim. Acta 413 (2000) 71.
[16] M.W. Shinwari, D. Zhitomirsky, I.A. Deen, P.R. Selvaganapathy, M.J. Deen, D. Landheer, Sensors 10 (2010) 1679.
[17] X. Li, A.J. Bard, Electroanal. Chem. J. 628 (2009) 35.
[18] Y. Kitamura, T. Uzawa, K. Oka, Y. Komai, H. Ogawa, N. Takizawa, H. Kobayashi, K. Tanishita, Anal. Chem. 72 (2000) 2957.
[19] T. Ezashi, P. Das, R.M. Roberts, Proc. Natl. Acad. Sci. USA 102 (2005) 4783.
[20] C.M. Cameron, F. Harding, W.S. Hu, S. Kaufman, Exp. Biol. Med. 233 (2008) 1044.
[21] K.L. Covello, J. Kehler, H.W. Yu, J.D. Gordan, A.M. Arsham, C.J. Hu, P.A. Labosky, M.C. Simon, B. Keith, Genes Dev. 20 (2006) 557.
[22] F. Xu, B. Sridharan, S.Q. Wang, U.A. Gurkan, B. Syverud, U. Demirci, Biomicrofluidics 5 (2011) 022207.
[23] R. Tripathi, H.K. Saini, R. Rad, C. Abreu-Goodger, S. van Dongen, A.J. Enright, Gene Expression Patterns 11 (2011) 334.
[24] M. Chen, Y.Q. Lin, S.L. Xie, H.F. Wu, J.F. Wang, Biotechnol. Lett. 33 (2011) 853.
[25] T. Matsue, S. Koike, I. Uchida, Biochem. Biophys. Res. Commun. 197 (1993) 1283.
[26] H. Shiku, T. Shiraishi, S. Aoyagi, Y. Utsumi, M. Matsudaira, H. Abe, H. Hoshi, S. Kasai, H. Ohya, T. Matsue, Anal. Chim. Acta 522 (2004) 51.
[27] Y.S. Torisawa, T. Kaya, Y. Takii, D. Oyamatsu, M. Nishizawa, T. Matsue, Anal. Chem. 75 (2003) 2154.
[28] Y.S. Torisawa, N. Ohara, K. Nagamine, S. Kasai, T. Yasukawa, H. Shiku, T. Matsue, Anal. Chem. 78 (2006) 7625.
[29] H. Shiku, S. Goto, S. Jung, K. Nagamine, M. Koide, T. Itayama, T. Yasukawa, T. Matsue, Analyst 134 (2009) 182.
[30] K. Inoue, P. Ferrante, Y. Hirano, T. Yasukawa, H. Shiku, T. Matsue, Talanta 73 (2007) 886.
[31] P. Liljeroth, C. Johans, C.J. Slevin, B.M. Quinn, K. Kontturi, Electrochem. Commun. 4 (2002) 67.
[32] P. Liljeroth, C. Johans, C.J. Slevin, B.M. Quinn, K. Kontturi, Anal. Chem. 74 (2002) 1972–1978.